- Polycyclic aromatic hydrocarbons (PAHs) in soils from a shale gas
- 2 exploitation area in China: Quantitative sources and risk analysis using an
- 3 improved hybrid model
- 4
- 5 Junwu Xiong<sup>1,2,3,4</sup>, Xi Fan<sup>1,3,4</sup>, Xiuwen Yang<sup>1,3,4</sup>, Huanfang Huang<sup>2,4\*</sup>, Chaojie Qin<sup>5</sup>, Chang Pu<sup>4</sup>,
- 6 Yuan Zhang<sup>4</sup>, Dacong Yin<sup>6</sup>, Wei Liu<sup>5</sup>, Shihua Qi<sup>1,3,4</sup>, Kevin C. Jones<sup>7</sup>, Wei Chen<sup>1,3,4,5,7,8\*</sup>
- 7
- 8 <sup>1</sup> School of Environmental Studies and MOE Key Laboratory of Groundwater Quality and Health, China
- 9 University of Geosciences, Wuhan 430078, China
- 10 <sup>2</sup> South China Institute of Environmental Sciences, Ministry of Ecology and Environment, Guangzhou
- 11 510535, China
- 12 <sup>3</sup> Hubei Key Laboratory of Yangtze Catchment Environmental Aquatic Science, China University of
- 13 Geosciences, Wuhan 430078, China
- <sup>4</sup> State Key Laboratory of Geomicrobiology and Environmental Changes, China University of Geosciences,
- 15 Wuhan 430078, China
- <sup>5</sup> Institute of Natural Resource Survey, China University of Geosciences, Wuhan 430074, China
- 17 <sup>6</sup> Hubei Key Laboratory of Water Resources & Eco-Environmental Sciences, Changiang River Scientific
- 18 Research Institute, Wuhan 430010, China
- <sup>7</sup> Lancaster Environment Centre, Lancaster University, Lancaster, LA1 4YQ, UK
- <sup>8</sup> Hubei Key Laboratory of Mine Environmental Pollution Control and Remediation, Hubei Polytechnic
- 21 University, Huangshi 435003, China
- 22 \* Corresponding authors.
- Emails: <u>huanghuanfang@scies.org</u> (HHF) and <u>wei.chen@cug.edu.cn</u> (CW).

### **ABSTRACT**

24

25

27

29

31

40

41

The environmental implications and risks of polycyclic aromatic hydrocarbons (PAHs) emitted from 26 shale gas exploitation to surrounding soils are not clear. In this study, concentrations of 16 priority-PAHs in soils of different land-use types from the Fuling shale gas exploitation area in Chongging, the first commercial shale gas exploitation area in China established in 2013, were analysed by a gas 28 chromatograph coupled with mass spectrometer (GC-MS). For the first time, the sources and risks of PAHs were systematically characterised by an integrated approach, combining multiple fractal 30 inverse distance weighting and concentration-area model, the absolute principal component multiple 32 linear regression model and Monte Carlo simulation. The average concentrations of 16 priority-PAHs in shale gas field soils (184 ng·g<sup>-1</sup>) were higher than in background forest/grasslands (73.4 33 ng·g<sup>-1</sup>) and in blowout land soils (56.4 ng·g<sup>-1</sup>). Environmental geochemical maps showed that PAH 34 hotspots were formed around towns and shale gas field sites, emphasising the dominant role of 35 anthropogenic activities over soil physicochemical properties in PAH accumulation. Coal 36 37 combustion/vehicle emissions and petrogenic sources are the major sources in the study area, 38 contributing 41% and 59% of the total PAHs, respectively. Notably, the source-oriented risk 39 assessment demonstrated that the ecological and health risks associated with petrogenic PAHs obviously exceeded those from coal combustion/vehicle emissions. The improved hybrid model can effectively quantify both PAH emission levels from shale gas exploitation activities and potential 42 risks from distinct sources This study highlights the impact of shale gas exploitation and provides a robust theoretical foundation for developing targeted strategies to mitigate PAH pollution risks in 43 44 shale gas exploitation areas.

45

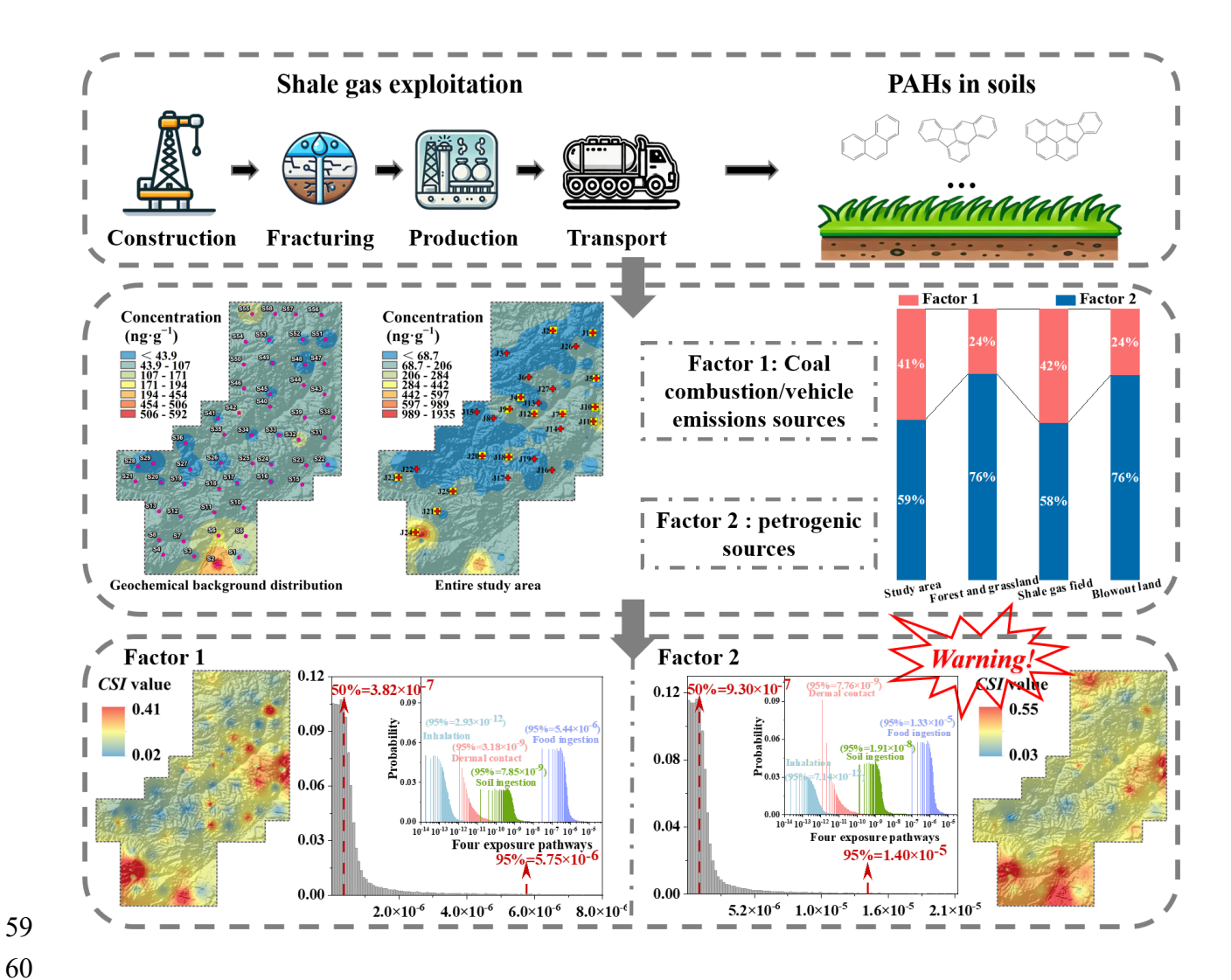
- 46 Keywords: Polycyclic aromatic hydrocarbons (PAHs), Shale gas, Source apportionment, Risk
- 47 assessment

48

## **Environmental Implication**

The rapid expansion of shale gas exploitation has raised global concerns about its environmental impact in recent years. In China, limited data on the long-term effects of pollutants from shale gas activities on surrounding soils creates uncertainty for effective policymaking. For the first time, this study employed a novel hybrid model to characterise the concentrations, sources and source-specific risks of 16-priority polycyclic aromatic hydrocarbons (PAHs) in soils from a shale gas exploitation area. The findings offer valuable insights for mitigating the adverse environmental and public health effects of PAHs and support the sustainable development of the shale gas industry.

# 58 Graphical Abstract



## 1. Introduction

61

62

63

64

65

66

67

68

69

70

71

72

73

74

75

76

77

78

79

80

81

Shale gas is an unconventional form of natural gas trapped in the pores and fractures of shale reservoirs, and its increased exploitation has triggered a shift in the global energy landscape<sup>1, 2</sup>. Possessing the world's largest shale gas reserves, China has rapidly expanded its production and become the third-largest global producer<sup>3</sup>, despite commencing its development approximately a decade later than the United States (US). The entire shale gas exploitation life cycle consumes substantial amounts of materials and energy, and can lead to considerable environmental impacts during well construction, hydraulic fracturing, and gas production<sup>4-8</sup>. One major concern is the release of organic pollutants, including polycyclic aromatic hydrocarbons (PAHs) during the construction and exploitation process<sup>9</sup>. PAHs have been widely detected in the air<sup>10</sup>, flowback and produced water<sup>11</sup> and oil-based drilling cuttings<sup>12</sup> in shale gas fields, and in surrounding watersheds and sediments<sup>13</sup>. PAHs, a class of petroleum by-products, are known for their high toxicity, carcinogenicity, and mutagenicity<sup>14</sup>. Chen et al. (2024) found that the carcinogenicity and ecotoxicity of organic pollutants in flowback water during production in China are 10<sup>3</sup> times higher than in the US<sup>15</sup>. PAHs in the environment are primarily the results of human activities such as vehicle emissions, petroleum spills, and fossil fuel combustion<sup>16</sup>. Due to their semi-volatility and long half-lives, PAHs can undergo long-range transport through both the atmosphere and water, leading to their widespread distribution across various environmental media<sup>17</sup>. PAHs are hydrophobic and tend to migrate to non-aqueous phases, particularly organic and particulate phases<sup>18</sup>, making soils the main environmental sink<sup>19</sup>. Most existing environmental impact assessments of shale gas exploitation focus solely on PAHs in the waste matrices generated during the process (such as flowback water<sup>11</sup> and oil-based drilling cuttings<sup>12</sup>), often overlooking the impact of PAHs released throughout the entire shale gas exploitation lifecycle on the surrounding soils. To mitigate the hazards posed by PAHs, further investigation into their sources and risks in soils is essential, particularly through source-oriented ecological and health risk assessments.

82

83

84

85

86

87

88

89

90

91

92

93

94

95

96

97

98

99

100

101

102

Geostatistical analysis and receptor models are commonly used to characterize PAH contamination<sup>20, 21</sup>. Traditional geostatistical methods for analysing the spatial distribution of PAHs, such as Kriging and inverse distance weighting (IDW) tend to smooth anomalous geochemical data when addressing local variations, which is not conducive to distinguishing between background and anthropogenic values<sup>22</sup>. The distinction between natural background and anthropogenic concentrations in environmental matrices is essential for the accurate quantification of pollution levels and the development of guidelines for environmental legislation<sup>23, 24</sup>. Cheng (1999)<sup>25</sup> developed a multiple fractal IDW (MIDW) model for geochemical mapping and a concentrationarea (C-A) model for concentration partitioning, which helps distinguish mineralization-related anomalies from background geological values, improving the accuracy of mineral searches. The absolute principal component score (APCS) model, which incorporates with multivariate linear regression (MLR), namely APCS-MLR, is an enhancement of principal component analysis (PCA)<sup>26</sup>. This receptor model can identify and quantify pollution sources and predict contaminant concentrations with limited available data<sup>27</sup>. Given the carcinogenic nature of some PAHs, numerous studies have evaluated their health risks<sup>28</sup>. However, previous studies conducted risk assessment based only on the levels of PAHs, neglecting the differences in risk posed by different sources, which are the critical basic information for implementing risk control of pollutants. The key contribution

of this study lies in uncovering the impacts of shale gas exploitation activities on the surrounding soil environment, identifying potential influencing factors, and offering a comprehensive, source-based quantitative assessment of the associated risks. With these considerations, for the first time, a hybrid model was introduced to assess the risk associated with source-orientated PAHs in soils from the Fuling shale gas exploitation area in Chongqing, Southwestern China.

The primary objectives of this study are: (1) to examine the distribution characteristics of PAHs in the study area, (2) to identify and attribute possible sources of PAHs to different land-use soil types using correlation analysis and improved receptor model, and (3) to evaluate the potential ecological and human health risks posed by the major PAH sources based a developed source-oriented risk assessment model. For the first time, the findings of this study are critical in providing insights into the extent of PAHs emissions from shale gas exploitations, assessing the hazards linked with various sources, and improving pollution prevention and control strategies for the shale gas industry.

#### 2. Materials and methods

#### 2.1 Study area

The study area is located in the eastern Fuling District, Chongqing, Southwestern China, characterized by a humid subtropical monsoon climate with an average annual temperature of 18.2 °C. Topographically, it exhibits a typical karst landscape of the Sichuan Basin, featuring thin soil layers<sup>29</sup>. The region primarily comprises an agroforestry ecosystem, with irregular patches distributed across flat to gently sloping terrain. The main crops cultivated in the area are rice and maize, although the total cultivated area is relatively small. The Fuling shale gas field, located within

this area, is a pioneer in China's shale gas exploitation and development, and it remains one of the largest shale gas fields outside North America<sup>30</sup>. Since its construction in 2013, shale gas exploitation activities have been continuously conducted in the area. As of December 2021, a total of 650 wells were put into operation in the Fuling shale gas field, yielding a cumulative gas production of 41.66 billion m<sup>3</sup>, and cumulative proven shale gas reserves of 897.5 billion m<sup>3</sup> <sup>31</sup>.

#### 2.2 Sample collection and chemical analysis

Soil samples of three land-use types were collected in August 2022: forests/grasslands, which are distant from shale gas exploitation and residential zones, representing the background of the study area; shale gas fields near centralized shale gas exploitation, production, and transportation sites (typically ca. 100 m × 100 m); and blowout lands adjacent to blowout pool (~30 m²), which are designed to collect and treat blowout fluids to prevent contamination and ensure safety during well testing or fracturing. A 2.5 km × 2.5 km sampling grid was established according to shale gas infrastructure distribution and study area dimensions (Fig. 1). Composite soil samples were formed from four sub-samples within a 50 m diameter for background sites, and from nearest soils outside the 4 borders of centralized facilities for shale gas field sites and blowout pool sites.

A total of 96 soil samples were collected: 54 for forests/grasslands, 27 for shale gas fields, and 15 for blowout lands (**Fig. 1**). Soil was collected to a depth of 0–20 cm, after removing vegetation and other debris from the surface. Samples were wrapped with pre-cleaned aluminum foil, sealed in polyethylene bags, and stored in 4 °C. The samples were then transported to the laboratory, immediately stored in a freezer at –20 °C until further analysis.

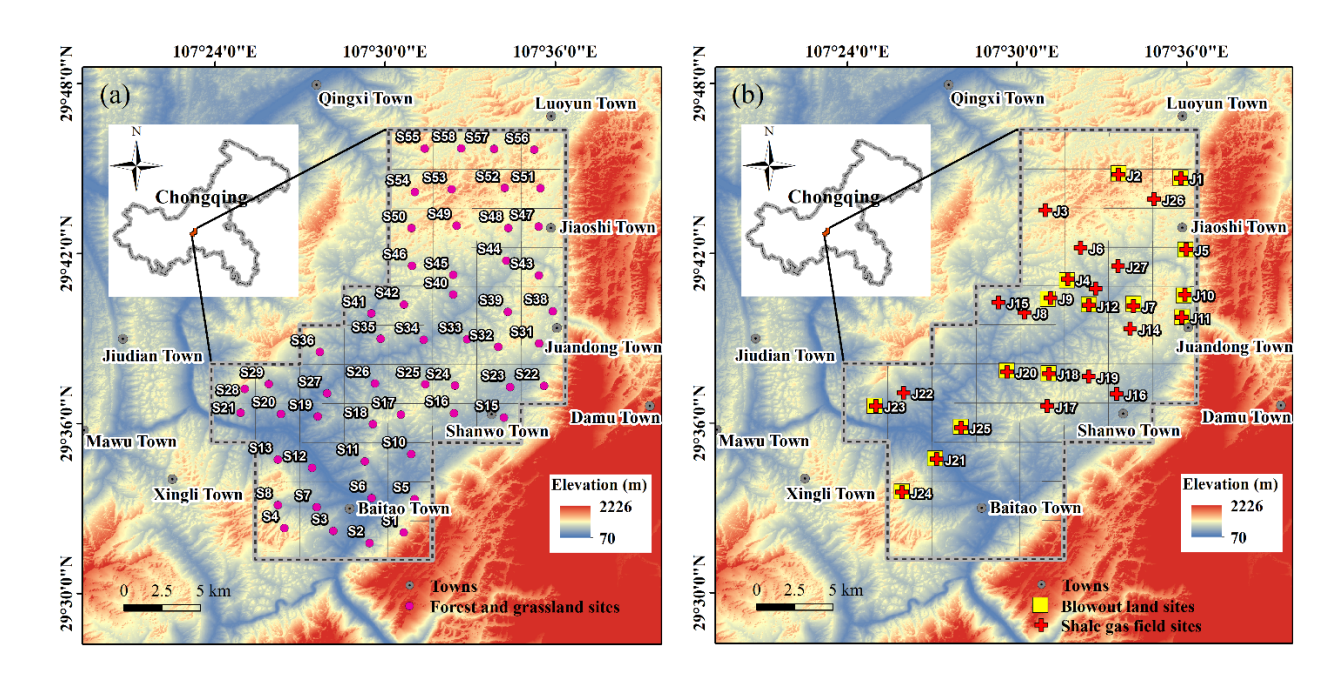


**Fig. 1.** Sampling sites of soil samples for three land use types in the study area: forests and grasslands (a), and shale gas fields and blowout lands (b)

The sixteen priority-PAHs (*Supplementary materials* **Table S1**, chemical information was provided in **Text S1**), namely Naphthalene (Nap), Acenaphthylene (Acy), Acenaphthene (Ace), Fluorene (Flu), Phenanthrene (Phe), Anthracene (Ant), Fluoranthene (Fla), Pyrene (Pyr), Benz[a]anthracene (BaA), Chrysene (Chr), Benzo[b]fluoranthene (BbF), Benzo[k]fluoranthene (BkF), Benzo[a]pyrene (BaP), Indeno(1,2,3-d)pyrene (IcdP), Dibenzo(a,h)anthracene (DahA) and Benzo(ghi)perylene (BghiP) in the soils were pre-treated and instrumentally analysed following established procedures from previous studies<sup>32,33</sup>, with further details provided in **Text S2**. Briefly, 10 g of freeze-dried soil samples were mixed with anhydrous sodium sulphate, spiked with 1000 ng of recovery surrogates (5 deuterated PAH compounds), and extracted with 160 mL of dichloromethane in a Soxhlet extractor at 45 °C for 24 hours, with copper flakes added for desulfurization. The extract was then concentrated and solvent-exchanged to *n*-hexane via rotary evaporation to 2–3 mL. Purification was performed using a multi-layer column (silica gel/neutral

alumina/anhydrous sodium sulphate, v:v:v = 6:3:1), eluted with 40 mL of dichloromethane/n-hexane (v:v = 2:3). The sample was concentrated to  $\sim 0.5$  mL and then transferred to a 2 mL brown sample glass vial using isooctane. The sample was further concentrated to 0.2 mL under high purity nitrogen (>99.999%), with 5  $\mu$ L of 200 mg·L<sup>-1</sup> hexamethylbenzene added as the internal standard.

The 16 target PAHs were analysed using an Agilent 6890N gas chromatograph coupled with a 5975 mass spectrometer (GC-MS), operated in 70 eV electron ionization and selected ion monitoring mode. 1 μL aliquot of each sample was injected at splitless mode into the GC-MS to separate 16 PAHs using a DB-5MS capillary column (30 m × 0.25 mm diameter, 0.25 μm film thickness, Agilent) with the following temperature program: initial temperature of 80 °C held for 2 min, increased to 180 °C at 10 °C·min<sup>-1</sup>, then to 290 °C at 4 °C·min<sup>-1</sup> and held for 13 min, with a total run time of 52.5 min. The injector and detector temperatures were 280 °C, with high purity helium as the carrier gas at 1.0 mL·min<sup>-1</sup>. Methods for analysing soil total organic carbon (TOC), pH and soil texture are described in Text S3. Detailed information regarding the chemicals used can be found in Text S1.

# 2.3 Quality assurance (QA) and Quality control (QC)

Quality assurance and quality control (QA/QC) procedures were conducted during the field sampling, and sample pre-treatment and analysis, the details were given in **Text S2**. In brief, blank (field, laboratory and solvent) and parallel samples were set, deuterated PAH compounds were spiked as recovery surrogates before pre-treatment, and QC standards were analysed daily. No obvious peaks were detected in the blank samples, relative standard deviations for target PAHs in parallel samples were <30%. Recoveries for deuterated PAH compounds ranged from  $53.5 \pm 17.5\%$  (Naphthalene-d<sub>8</sub>) to  $103 \pm 26.8\%$  (Chrysene-d<sub>12</sub>), and method detection limits (MDLs) for 16 PAHs

in soil were  $0.01-1.07 \text{ ng} \cdot \text{g}^{-1}$  (**Table S1**).

## 2.4 Improved hybrid models for source-specific risk assessment

The operational framework of the improved hybrid model is illustrated in **Fig. S1**. Firstly, PAH concentrations of field soil samples from different land-use types were analysed and acquired. Geochemical maps were then generated by MIDW and C-A models. Sources were identified and quantified through molecular diagnostic ratio (MDR) and APCS-MLR. Finally, potential ecological and human health risks were assessed by integrating source-specific pollution status combined with contamination severity index (*CSI*) and with Monte Carlo simulated incremental lifetime cancer risks (*ILCRs*), respectively.

#### 2.4.1 Environmental geochemical cartography

Environmental geochemical maps of PAHs were generated by the GeoDAS<sup>TM</sup> software, applying the MIDW computational display, which preserves information on local variability<sup>22</sup>. The concentration intervals in the MIDW interpolation map are segmented using the C-A method, which plots the pixel concentration values against the cumulative area in double logarithmic coordinates<sup>25</sup>. Briefly, the area concentration  $[A(\sigma)]$  is related to the concentration of elements greater than  $\sigma$  in a power rate relationship. If the geochemical surface is fractal, a linear relationship is observed, whereas for multifractal surfaces, the values follow multiple distinct linear relationships. The transition points between these linear relationships serve as cut-off points, allowing the division of geochemical values into different components. These maps, therefore, reflect not only the frequency distribution of pixel values but also the spatial and geometric properties of the pixel regions. In this study, the environmental geochemical maps of PAHs generated by the MIDW and C-A models help

differentiate between areas representing natural backgrounds and those disturbed by human activities. For further details on the calculations, refer to previous studies<sup>22, 25</sup>. The results of the C-A model of the 16 PAHs in this study are shown in **Fig. S2**.

### 2.4.2 Molecular diagnostic ratio (MDR)-assisted APCS-MLR source identification

The PAH sources are usually identified by the MDR method, mainly based on the ratios of Ant/(Ant + Phe), Fla/(Fla + Pyr), BaA/(BaA + Chr), and IcdP/(IcdP + BghiP)<sup>27, 34</sup>. Details of the sources indicated by the ratios are shown in **Text S4**.

The APCS-MLR receptor model was improved on PCA, with the key modification being the artificial introduction of samples with a value of 0 to normalise the data. APCS scores were calculated by subtracting principal factor scores with a value of 0 from the principal factor scores obtained in the PCA analyses<sup>35</sup>. Following the determination of the number of potential sources (APCS score), the contribution (%) of each source to each component was calculated by MLR. Details of the improved APCS-MLR receptor model are given in previous studies<sup>35, 36</sup>, and the specific calculations in this study are given in **Text S4**.

#### 2.4.3 Ecological risk assessment

The contamination severity index (*CSI*) was used to evaluate the ecological risk of soils in the study area. The index structure is based on the effect range low (ERL) and effect range median (ERM) of effect intervals reported in previous studies<sup>26, 36</sup> to serve as boundaries for biota and non-utilisation impacts (**Table S1**). These two effect values classify concentrations into three ranges: concentrations below the ERL indicate a low ecological risk with less than a 10% probability of adverse effects; concentrations between the ERL and ERM suggest an occasional ecological risk;

and concentrations equal to or above ERM indicate a frequent ecological risk, with a probability of adverse effects exceeding 50%<sup>26</sup>. The method assigns different weights according to the concentration ratios of pollutants to more accurately express the ecological risk of soil, which was calculated as shown in eq 1<sup>26</sup>:

$$CSI = \sum_{i=1}^{n} W_{i} \left[ \left( \frac{C_{i}}{ERL_{i}} \right)^{\frac{1}{2}} + \left( \frac{C_{i}}{ERM_{i}} \right)^{2} \right]$$
 (1)

Where  $C_i$  was the measured value of individual PAH (ng·g<sup>-1</sup>),  $W_i$  represents the weight of pollutant i, calculated as the PCA/factor analysis of the pollutant (**Table S2**), considering only anthropogenic pollution factors (eq 2).

230 
$$W_{i} = \frac{(L_{fi} \times E_{v})}{\sum_{i=1}^{n} (L_{fi} \times E_{v})}$$
 (2)

where  $L_{fi}$  and  $E_{v}$  represent the factor loadings and eigenvalues of pollutant i, respectively.

#### 2.4.4 Human health risk assessment

232

233

234

235

236

237

238

239

240

241

In this study, the concentrations of seven carcinogenic PAHs (BaA, BaP, BbF, BkF, Chr, DahA, and IcdP) in soil were converted to toxic equivalents based on BaP (*TEQ*<sub>BaP</sub>, seeing **Text S5**), and the *ILCR* model was used to quantitatively assess the carcinogenic risk of PAHs<sup>37</sup>. *ILCR* values were calculated for children (1–11 years old), teenagers (12–17 years old) and adults (18–70 years old) based on four exposure pathways: soil ingestion, food ingestion, dermal contact and inhalation. Detailed assessment methods are provided in **Text S5**.

To address the uncertainties inherent in the *ILCR* model, this study employed Monte Carlo simulation methods to minimize these uncertainties and optimize the accuracy of health risk assessment<sup>36</sup>. Briefly, the Monte Carlo simulation method uses the probability distributions of the

parameters in the *ILCR* model to reduce uncertainty. Unlike traditional fixed-value methods, this method incorporates a range of possible parameter values, each with an associated probability distribution function. By generating random values for these parameters during the simulation, the method covers a wide range of possible scenarios and provides a robust and comprehensive solution to the research objectives. Oracle Crystal Ball 11.1.2.4 was used in this study. Each run consisted of 50,000 iterations and a confidence level of 95%. **Table S3** provides detailed information on the distributions and values of the parameters used in the Monte Carlo simulation.

#### 2.5 Statistical analysis

For statistical analyses, concentrations below the MDLs were substituted by the values of 1/2 MDLs (Table S1). Due to the data's deviation from normal distribution (as indicated by the Kolmogorov-Smirnov test, p < 0.05), nonparametric tests were used for significance analyses. Spearman's correlation coefficient was used to assess the relationship between PAH concentrations and soil properties. All statistical analyses were conducted using IBM *SPSS* Statistic 27.

#### 3. Results and discussion

### 3.1 Occurrence and distribution characteristics of PAHs

#### 3.1.1 Entire study area

The total concentrations of 16 PAHs ( $\sum_{16}$ PAHs) in the study area ranged from 11.5 to 1798 ng·g<sup>-1</sup>, with an average of 105 ng·g<sup>-1</sup> (**Fig. 2a** and **Table S4**). Only two studies reported PAH concentrations in soils around shale gas exploitation areas: The average  $\sum_{16}$ PAHs concentrations in the Sichuan Basin (370 ng·g<sup>-1</sup>)<sup>38</sup> and the Chongqing exploitation area (348 ng·g<sup>-1</sup>)<sup>39</sup> were slightly higher than those in present study. Given the fact that both studies considered only single soil types

and small sample sizes (<20), we recommend that the results of the comparisons need to be viewed with caution. According to the classification of soil PAH contamination by Maliszewska-Kordybach <sup>40</sup>, over 94.8% % of soil samples in this study were categorized as non-contaminated (<200 ng·g<sup>-1</sup>), while heavily contaminated sites (>1000 ng·g<sup>-1</sup>) accounted for only 0.01 % of samples (one sample). Based on the Chinese soil environmental standard GB 36600-2018<sup>41</sup> for development land and GB 15618-2018<sup>42</sup> for agricultural land, all the concentrations for the individual PAHs in this study area were below the regulatory limits, which prescribes screening values of 25,000 ng·g<sup>-1</sup>, 490,000 ng·g<sup>-1</sup>, 5,500 ng·g<sup>-1</sup>, 5,500 ng·g<sup>-1</sup>, 55,000 ng·g<sup>-1</sup>, 550 ng·g<sup>-1</sup>, 550 ng·g<sup>-1</sup> and 550 ng·g<sup>-1</sup> for Nap, Chr, BaA, BbF, BkF, BaP (only BaP restricted among PAHs for agricultural land, but the same value for development land), IcdP and DahA, respectively.

Compared to conventional natural gas and crude oil exploitation areas, the average  $\sum_{16}PAHs$  concentration (105 ng·g<sup>-1</sup>) in the study soils were lower than that in the Daqing oil field (2240 ng·g<sup>-1</sup>)<sup>43</sup> and the Yellow River Delta oil field (383 ng·g<sup>-1</sup>)<sup>44</sup>, but comparable to that in the Shengli oil field (160 ng·g<sup>-1</sup>)<sup>45</sup>. This difference from conventional oil and gas fields is expected, as shale gas exploitation (~10 years) is still at an early stage. Seven carcinogenic PAHs ( $\sum_{7}PAHs$ , including BaA, BaP, BbF, BkF, Chr, DahA and IcdP) accounted for avg. 49.2% of the  $\sum_{16}PAHs$ , with an average of 51.4 ng·g<sup>-1</sup>. Phe (12.7%), IcdP (12.6%), BbF (12.3%), BghiP (11.9%) and Chr (10.3%) presented higher concentrations compared to other PAHs (**Fig. 2b**), similar to those found in soils from crude oil exploitation areas<sup>43</sup> or crude oil industrial regions<sup>36</sup>.

Using a Monte Carlo method<sup>37</sup> (details in **Text S6**), the  $\sum_{16}$ PAHs inventories in soils across the study area were estimated to range from 2.29 to 6.23 tons (average 3.53 tons) (**Fig. S3**). The mass

inventory of ∑16PAHs per unit area was then calculated in order to reasonably compare among different areas. The average mass inventory of ∑16PAHs per unit area (10.5 kg·km<sup>-2</sup>) in the Fuling study area was lower than that of the densely populated Shenzhen, China (19.6 kg·km<sup>-2</sup>)<sup>46</sup>, but higher than that of Caserta province, Italy (2.81 kg·km<sup>-2</sup>)<sup>37</sup>, suggesting the necessity to quantify PAH emissions from construction and exploitation activities in emerging shale gas production areas.

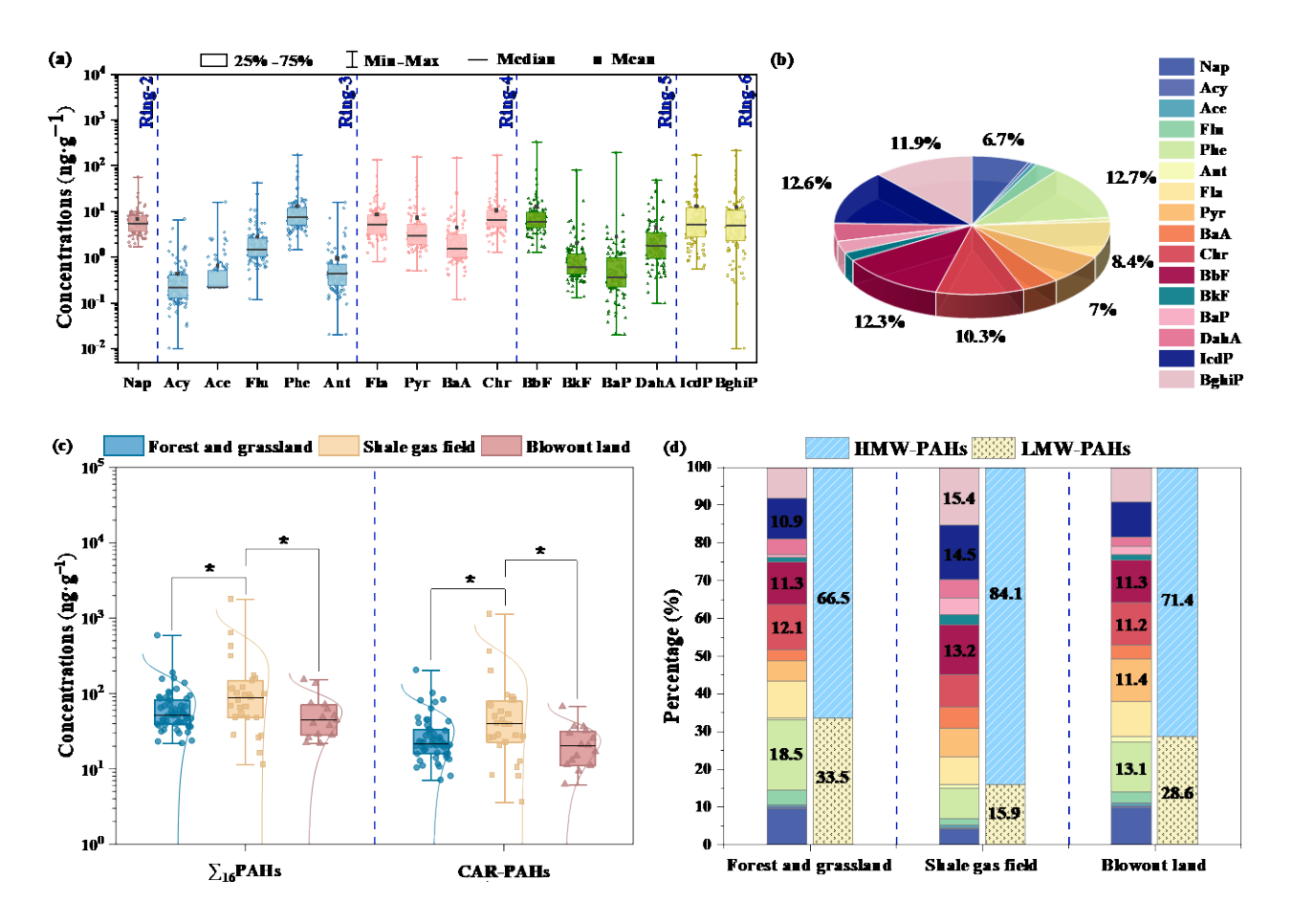


Fig. 2. Concentrations (a) and composition (b) of 16 PAH monomers in the study soils, comparisons of  $\sum_{16}$ PAHs and CAR-PAHs: sum of 7 carcinogenic PAHs (c), and compositions of 16 PAH monomers and high-molecular-weight (HMW)-PAHs and low-molecular-weight (LMW)-PAHs (d) in soils among three land-use types. \*: p < 0.05 (Mann-Whitney U test).

The coefficients of variation (CV) of individual compounds in this study ranged from 73.0%

to 450% (average 138%, **Table S4**), indicating that all PAH compounds have a highly variable spatial distribution. The study area was a typical shale gas exploitation area, extensive transportation and industrial activities were key sources of disturbance. These human activities widely released PAHs, which diffuse through various media and are deposited at different locations. Environmental geochemical maps representing the spatial distribution of PAHs were generated by the MIDW model and partitioned with the C-A method (**Figs. 3a-b** and **S4**). The hotspots of PAHs throughout the study area were mainly in shale gas exploitation (989–1935 ng·g<sup>-1</sup>) and in residential town areas (597–989 ng·g<sup>-1</sup>), indicating the impact of human activities on PAHs in the environment. Similarly, a study in Naples, Italy<sup>47</sup> found hotspots of PAHs concentrated in urban areas, and Zhang et al. (2023)<sup>48</sup> found higher concentrations of PAHs in soils near the coke plants than in other areas, driven by coke calcination and raw material leakage.

Further analysis of the relationship between soil PAH concentrations and soil properties, including pH, TOC, and soil texture (**Fig. 3c**), was conducted to better understand the factors influencing PAH spatial distribution. The significant correlation between pollutants indicates they may share common or similar sources (emissions) and/or exhibit similar environmental behaviours<sup>34</sup>, <sup>49</sup>. In this study, significant positive correlations were observed among PAHs (**Fig. 3c**, between 2-ring and 6-ring PAHs at 0.01 significance level, and between all other combinations of individual components of PAHs at 0.001 significance level). Considering the differences in physicochemical properties among PAHs with varying ring numbers (**Table S1**), this suggested these different individual components of PAHs may originate from similar sources or emissions. Soil physicochemical properties play a secondary regulatory role in shaping the distribution

characteristics of PAHs<sup>50</sup>. HMW-PAHs, characterized by low water solubility and volatility (Table S1), are typically readily adsorbed by soil organic matter (SOM), and finer soil particles with larger specific surface areas, such as silt and clay, provide more adsorption sites for PAHs<sup>51</sup>. Interestingly, significant positive correlations were observed between LMW-PAHs and both TOC and soil texture in this study (Fig. 3c). This may be due to LMW-PAHs being predominant in the gas phase, making them more readily adsorbed by SOM through air-soil interface exchange<sup>52-54</sup>. In contrast, HMW-PAHs are primarily bound to particles and enter the soil through dry or wet deposition, with their distribution governed by proximity to pollution sources, particle deposition rates and local emissions<sup>52, 55</sup>. Therefore, in the study area with intensive pollution sources, HMW-PAHs may exhibit a negative correlation with soil TOC (Fig. 3c). This observation is consistent with findings from studies on soils in traffic and industrial-intensive areas of Delhi (India)<sup>56</sup> and western Europe<sup>52</sup>. In summary, the spatial distribution of PAHs in the study area may be primarily driven by direct emissions from all the processes of shale gas exploitation (as sources identified in Section 3.2), rather than secondary redistribution regulated by soil properties.

#### 3.1.2 Different land-use types

316

317

318

319

320

321

322

323

324

325

326

327

328

329

330

331

332

333

334

335

336

The shale gas fields exhibited significantly higher concentrations (Mann-Whitney U test, p < 0.05) of both  $\sum_{16}$ PAHs and  $\sum_{7}$ PAHs (average of 184 ng·g<sup>-1</sup> and 99.1 ng·g<sup>-1</sup>, respectively) compared to the forest/grasslands ( $\sum_{16}$ PAHs: 73.4 ng·g<sup>-1</sup>,  $\sum_{7}$ PAHs: 31.7 ng·g<sup>-1</sup>) and blowout lands ( $\sum_{16}$ PAHs: 56.4 ng·g<sup>-1</sup>,  $\sum_{7}$ PAHs: 23.5 ng·g<sup>-1</sup>) (**Fig. 2c**). The elevated concentrations observed in this study indicated that shale gas exploitation activities have a widespread influence as the average concentration of  $\sum_{16}$ PAHs in background soils of nearby area during the same period was 55.8 ng·g<sup>-1</sup>

337  $^{32}$ .

338

339

340

341

342

343

344

345

346

347

348

349

350

351

352

353

354

355

356

Forest/grassland soils are considered as the background in the study area. To quantify the impact of shale gas exploitation activities on soil PAH concentrations in the study area, the ratios of soil PAH concentrations in shale gas fields to background were calculated within the same sampling grids (2.5 km×2.5 km, Fig. 1). The ratios for  $\Sigma_{16}$ PAHs were >1 for over 60% of the sampling grids, with median ratios ranging from 0.99 to 2.19 for individual PAHs (Fig S5). Notably, the ratios for BkF, BaP, and BghiP were >100 (Fig S5) in certain sampling grids. In terms of source characteristics, BkF and BaP are characteristic products of high-temperature incomplete combustion of fossil fuels<sup>57</sup>, which may be generated in large quantities by diesel generators, fracturing equipment, and heavy machinery widely used in shale gas exploitation<sup>4-8</sup>. Meanwhile, BghiP, a specific marker of trafficrelated emissions<sup>27</sup>, showed a notable increase in the shale gas field, reflecting frequent vehicle activities in the study area. Shale gas exploitation involves intensive energy consumption, including continuously operating drilling equipment, large-scale fracturing operations, and heavy vehicle transport of raw materials and products<sup>15</sup>. The spatial clustering of these energy-intensive activities around the shale gas field may serve as the principal driver of the enrichment of these PAH compounds. Additionally, the average proportion of HMW-PAHs (Fig. 2d) in shale gas fields (84.1%) and blowout sites (71.4%) was higher than that in forest/grassland areas (66.5%), further confirming that intensive industrial and transportation activities around shale gas fields have led to an increase in HMW-PAHs concentrations in soils<sup>52-54</sup>. These findings confirm that the distribution of HMW-PAHs is controlled by the distance from pollution sources, local emissions and particle deposition.

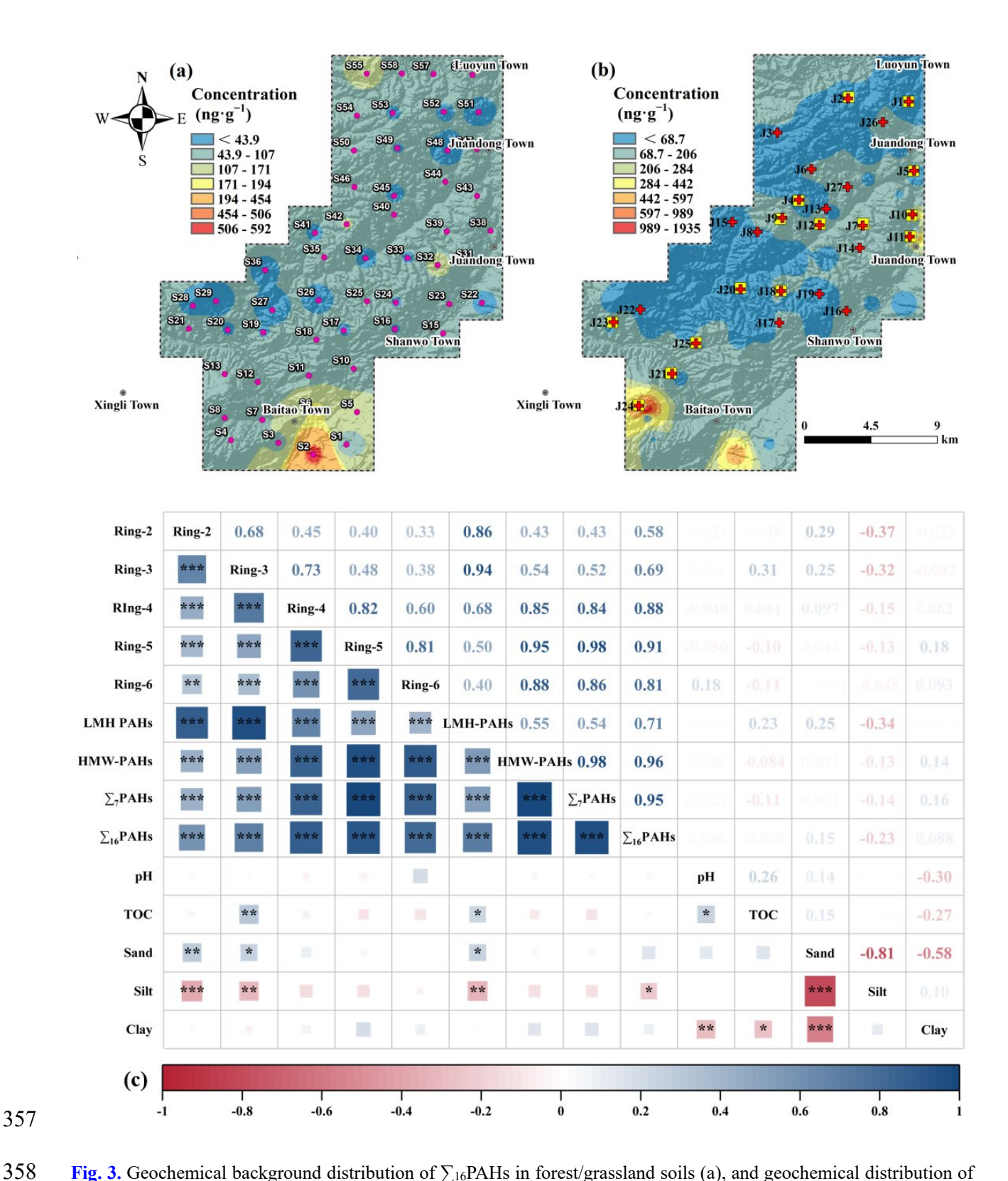


Fig. 3. Geochemical background distribution of  $\sum_{16}$ PAHs in forest/grassland soils (a), and geochemical distribution of  $\sum_{16}$ PAHs across the study area (b) mapped by MIDW and concentration partitioning by C-A method, and correlation analysis (c) between soil physicochemical factors and PAHs in soils (\* p < 0.05; \*\* p < 0.01; \*\*\* p < 0.001).

Significantly different (Kruskal-Wallis test, p < 0.001) CVs were found between shale gas fields (average 210%, range 73.0%–450%) and forest/grasslands (average 118%, range 64.2%–195%) and blowout lands (average 100%, range 36.0%–214%). Therefore, land use variations should be considered when studying soil PAHs from active industrial areas in the future, due to these notable differences. A comparison between the geochemical background distribution of PAHs (**Fig. 3a**) and the distribution across the entire study area (**Fig. 3b**) revealed that shale gas exploitation had increased PAH concentrations and altered the spatial distribution of PAH hotspots. Previously concentrated in towns, these hotspots have expanded to include both shale gas extraction fields and towns, highlighting the impact of shale gas exploitation on PAH distribution.

## 3.2 Source analysis of PAHs in soils

### 3.2.1 Source identification of PAHs using MDR

Generally, LMW-PAHs were the dominant PAH pollutants from petrogenic PAHs and incomplete combustion from biomass, while HMW-PAHs were the dominant pyrolytic PAHs (high-temperature combustion products of fossil fuels, coal, etc.)<sup>57-59</sup>. Sources of PAHs in soils were qualitatively identified using the MDR. The diagnostic ratio ranges (averages) of BaA/(BaA + Chr), Ant/(Ant + Phe), Fla/(Fla + Pyr) and IcdP/(BghiP + IcdP) in the study soils (Fig. 4a-b) were 0.084–0.465 (0.219), 0.004–0.194 (0.065), 0.115–0.875 (0.610) and 0.184–0.985 (0.559), respectively. Among the sampling sites, 45.8% of sampling sites fell within the range indicative of petrogenic sources, while 31.3% were within the combined range of petroleum combustion and petrogenic sources (Fig. 4a). Further classification (Fig. 4b) revealed that 61.5% of the sites were associated with biomass and coal combustion, whereas 29.2% fell within the combined range of

petroleum combustion and biomass/coal combustion sources. These findings suggested that petrogenic and combustion sources were the major PAH sources in the study area.

382

383

384

385

386

387

388

389

390

391

392

393

394

395

396

397

398

399

400

401

402

PAH sources in soils vary considerably across land-use types (Fig. 4a-b and Table S5), reflecting distinct emission profiles and energy consumption activities in different locations. Forest/grassland soils (64.8% sites fell within petrogenic source ranges) were more influenced by petrogenic sources than shale gas field (18.5%) and blowout land soils (26.7%) (Fig. 4a). Shale gas field sites had 33.3% from petroleum combustion and petrogenic sources, and 25.9% from biomass/coal combustion and pyrogenic sources (Fig. 4a). Blowout land sites had 33.3% from petroleum combustion and pyrogenic sources (Fig. 4a). This corresponded to the characteristics of elevated combustion activities from shale gas operations and blowout response, including gas flaring, diesel combustion from drilling/remediation equipment, and heavy vehicular traffic, resulting in more combustion-derived PAHs compared to forest/grassland areas. Fig. 4b revealed that 79.6% of the forest/grassland, 59.3% of the shale gas field, and 53.3% of blowout land sites fell within the biomass/coal combustion mixed sources area. This indicated that PAHs in the study area were primarily influenced by biomass/coal combustion. Additionally, 20.4% of forest/grassland, 29.6% of shale gas field and 40% of blowout land sites fell within the combined source range of biomass/coal combustion and petroleum combustion (Fig. 4b). This further supported the conclusion that shale gas fields and blowout lands were considerably more affected by combustion sources compared to forest/grassland soils. The apportioned source patterns of PAHs in soils across different land-use types were primarily shaped by the interplay of PAHs' inherent degradation rates, long-term production activities in the study area, and the cumulative impact of time. Over the past

decade, dominant shale gas exploitation and agricultural activities in the area were the major contribution of PAHs into the soils. The degradation rates of PAHs are molecular-weight-dependent: LMW-PAHs degrade more rapidly than HMW-PAHs<sup>60, 61</sup>. Compared with forest/grasslands, shale gas fields and blowout lands have received a greater influx of "fresh" PAHs from recent energy-consuming activities. The PAHs in soils from different land-use types across the study area have accumulated over a long period of time during combustion input/degradation. This finding aligns with our observations in *Section 3.1* (Fig. 2d), where shale gas field soils (84.1%) exhibited a greater proportion of HMW-PAHs compared to forest/grassland soils (66.5%).

### 3.2.2 Source identification of PAHs in soils using APCS-MLR model

The APCS-MLR model was further introduced to compensate for the inability of MDR and conventional PCA to quantitatively identify sources (Text S4). The Kaiser-Meyer-Olkin test and Bartlett's test with result values of 0.81 and p < 0.001, respectively, showed that the data were appropriate for APCS-MLR analyses.

Two principal components (PCs) were extracted with eigenvalues greater than 1 and accounted for 87% of the total variance in the data set (**Fig. 4c**). PCI explained 60.5% of the total variance and had high loadings of BaP (76.7%) and medium loadings of BkF (65.8%), BaA (62.2%), BghiP (59.3%), BbF (56.8%), IcdP (54.1%) and Pyr (52.5%). BaP, BkF, Pyr and BbF are the indicators of coal combustion, while IcdP, BghiP and BaA are recognized as indicators of vehicle emissions<sup>27, 33, 57</sup>. Thus, PCI was identified as mixed sources of coal combustion and vehicle emission, representing PAH emissions associated with the stable production stage of shale gas exploitation, characterized by substantial energy consumption and intensive transportation activities. PCII accounted for 26.5%

of the total variance and is dominated by Nap (93.3%), Acy (95.1%), Flu (89.2%), and Phe (93.4%). The main component of shale gas is methane. Methane combustion can only form PAHs with a maximum of four aromatic rings<sup>62</sup>, with Nap as the representative compound under certain combustion conditions<sup>63</sup>. Nicolini et al. (2015)<sup>64</sup> observed that PAHs with two to four aromatic rings are prevalent, with Phe being the most abundant in pyrolyzed shale materials. This may indicate the LMW-PAHs are released into the environment during emergency flaring when there is shale gas leakage. Additionally, correlation analysis revealed the homogeneity among PAHs with different ring numbers (Fig 3c), which was consistent with the simultaneous presence of shale gas fields at different development stages within the study area. Furthermore, Nap, Ace, Phe and Ant and their derivatives have been identified as the dominant PAHs in produced and formation water from shale gas exploitation areas throughout the US9. The formation of shale gas is a complex geological process, jointly influenced by the organic matter stored in the shale and the diagenesis<sup>65</sup>. Therefore, PCII was identified as a petrogenic source, consistent with the PAH sources detected in the air around natural gas exploitation wells in the US<sup>10</sup>. It may be primarily attributed to early-stage shale gas exploitation activities, encompassing drilling operations, hydraulic fracturing processes, and direct wellhead leakages. The MLR results further revealed that coal combustion/vehicle emission (Factor 1, F1) and

424

425

426

427

428

429

430

431

432

433

434

435

436

437

438

439

440

441

442

443

444

The MLR results further revealed that coal combustion/vehicle emission (Factor 1, F1) and petrogenic sources (Factor 2, F2) are potential sources of soil PAHs in the study area with an average contribution of 40.9% and 59.1% (Fig. 4d), respectively. Similar source patterns were found in the blowout lands and forests/grasslands. Drilling operations and frequent blowout activities during the initial stages of shale gas site construction may result in direct emissions of PAHs<sup>66</sup>. These direct

emissions were typically highly volatile LMW-PAHs (e.g., Nap and Phe, etc.) that readily volatilised throughout the study area and then settled into the soils<sup>10</sup>. Forests/grasslands are affected by the forest filter effect, i.e., the uptake of atmospheric POPs (including volatile PAHs) by foliage and their transport to the forest floor via litterfall, throughfall and the erosion of wax and particles<sup>67, 68</sup>. Different from blowout lands and forests/grasslands, coal combustion/vehicle emission contributed more (avg. 58.0%) to the PAHs in the shale gas fields. Once the gas production phase has stabilised, shale gas fields are accompanied by more human activities, including gas processing and transport (e.g. construction materials, water and products)<sup>9</sup>.

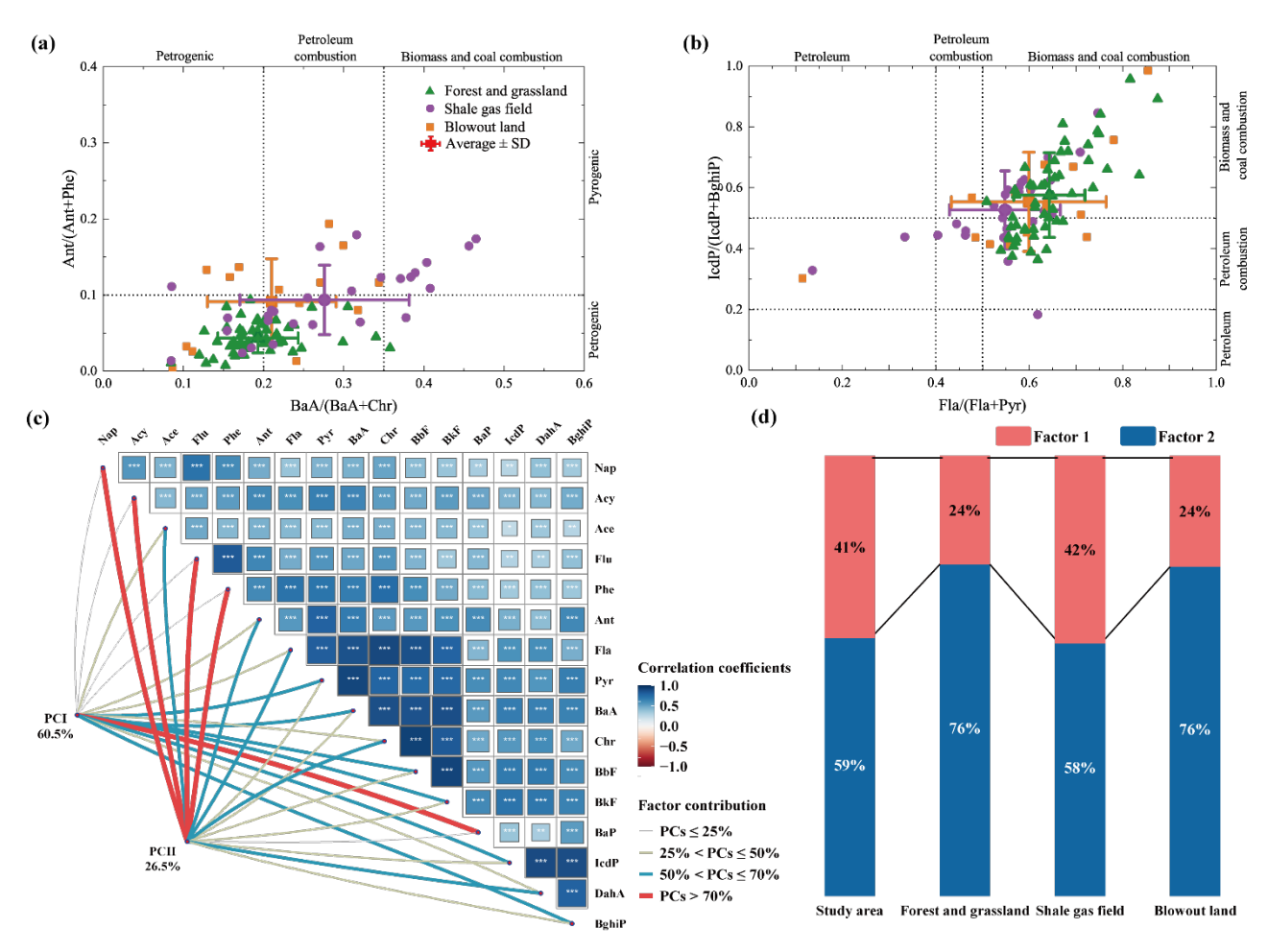


Fig. 4. Isomeric ratios of Ant/(Ant + Phe) and Fla/(Fla + Pyr) (a), and ratios of IcdP/(BghiP + IcdP) and BaA/(BaA + Chr) (b) in soils of different land-use types, determination of correlation between PAH monomers and sources

of contamination by combining Spearman's correlation analysis (\*p < 0.05; \*\*p < 0.01; \*\*\*p < 0.001) and APCS
MLR model (c), and contributions of each source of PAH in soils of different land-use types (d).

The APCS-MLR model showed excellent agreement with the results of MDR identification of sources. Notably, besides accurately quantifying the sources of PAHs, the APCS-MLR model also assisted in predicting the concentration of PAHs in the soils of the study area  $(0.69 < R^2 < 0.98, Fig. S6)$ .

# 3.3 Source-specific ecological risk assessment

The contamination severity index (CSI) values in the study area ranged from 0.10 to 0.92 with an average of 0.18 (**Table S6**). The shale gas fields had slightly higher CSI values than blowout lands and forest/grasslands. With all CSI values of < 0.5, PAHs in soils of forest/grassland and blowout land did not pose potential ecological risk (**Table S6**); and only one site in the shale gas fields displayed a low ecological risk (0.5 < CSI < 1).

The ecological risks of soil PAHs posed by different sources were subsequently identified by APCS-MLR (**Text S5**). Comparison of *CSI* values contributed from the two identified sources showed that coal combustion/vehicle emission (F1) contributed significantly (Mann-Whitney U test, p < 0.001) lower risk than petrogenic sources (F2): Average *CSI* values generated from F1 and F2 accounted for 33.3% and 66.7%, respectively. Average *CSI* values from petrogenic sources in the shale gas fields were on average 1.3 times higher than those from coal combustion/vehicle emissions and even averaged 3 times and 2.7 times higher in forests/grasslands and blowout lands, respectively. Spatial distribution *CSI* values revealed that high ecological risk areas were primarily concentrated at the interface zones between towns and shale gas fields (**Fig. 5a**). The highest risks

were identified in the south at the boundary between the Baitao Town and J24 Shale Gas Field, and in the east between the Jiandong Town and J11 Shale Gas Field. The *CSI* values for coal combustion/vehicle emission sources and petrogenic sources were in the ranges from 0.02 to 0.38 with an average of 0.06, and from 0.04 to 0.53 with an average of 0.12, respectively. Spatially, the ecological risks induced by coal combustion/vehicle emissions exhibited distinct localized distribution patterns, with risk hotspots mainly confined to towns and shale gas exploitation zones (Fig. 5b), whereas the ecological risks stemming from petrogenic sources more widely affect the entire study area (Fig. 5c). Despite the overall low ecological risks of soil PAHs in the study area, proactive establishment of a tiered regulatory monitoring framework is recommended when considering future expansion of shale gas exploitation areas and the accumulation properties of PAHs in soils: 1) implement routine monitoring in areas affected by petrogenic sources, 2) conduct targeted and intensive monitoring for high-risk areas where towns and shale gas fields interact, and 3) establish the prioritized risk management strategies for petrogenic PAHs.

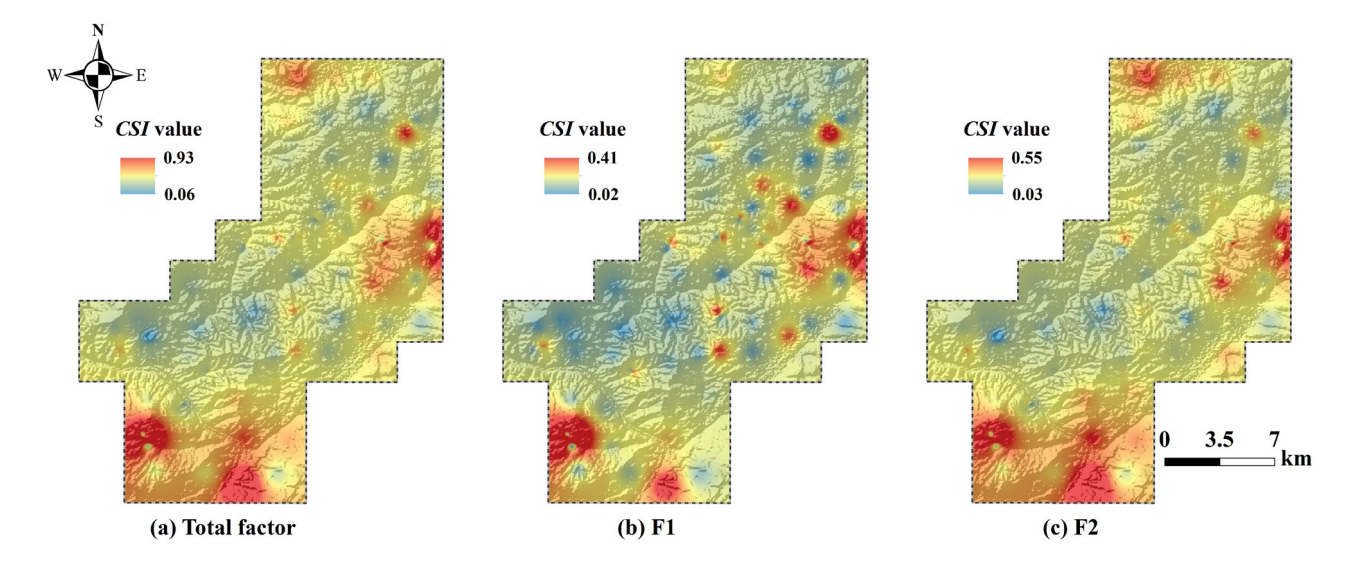


**Fig. 5.** Ecological risk distribution map based on all contributions (a), based on contributions of coal combustion and vehicle emission sources (F1, b), and based on petrogenic sources (F2, c) in the study area.

### 3.4 Source-specific health risk assessment

493

494

495

496

497

498

499

500

501

502

503

504

505

506

507

508

509

The concentration values of 7 carcinogenic PAHs were transformed using the  $TEQ_{BaP}$  method, to assess the carcinogenic risk of PAHs in soils through four exposure pathways with probabilistic modelling (Text S5). In terms of regulation, *ILCR* values  $< 10^{-6}$ ,  $10^{-6} \sim 10^{-4}$ , and  $> 10^{-4}$  indicate negligible, potential, and unacceptable cancer risks, respectively<sup>36, 69</sup>. The 95% percentile *ILCRs* values for the study area ranged from  $2.61 \times 10^{-6}$  (teenagers) to  $1.88 \times 10^{-5}$  (adults). There is potential carcinogenic risk across all ages, where the risk to adults is notably ~10 times higher than to children and teenagers (Fig. 6a-c). Among the four exposure pathways (soil ingestion, food ingestion, dermal contact and inhalation, in Text S5), the risk through food ingestion is several orders of magnitude higher than the other three exposure pathways. The higher PAH exposure for adults than children and teenagers might be attributed to a higher intake of vegetables and cereals<sup>37, 70</sup>. Thus, the carcinogenic risks associated with root vegetables, other vegetables, and cereals were further evaluated using a probabilistic model. Results (Table S7) confirmed that cereals posed higher ILCR than vegetables, across all three age groups, with the risk ranked adults  $(1.79 \times 10^{-5})$  > children  $(3.60\times10^{-6})$  > teenagers  $(2.32\times10^{-6})$ ; root vegetables posed the higher *ILCR* than other vegetables across all three age groups, with the risk ranked adults  $(1.15\times10^{-6})$  > children  $(7.30\times10^{-7})$  > teenagers  $(2.95 \times 10^{-7})$ .

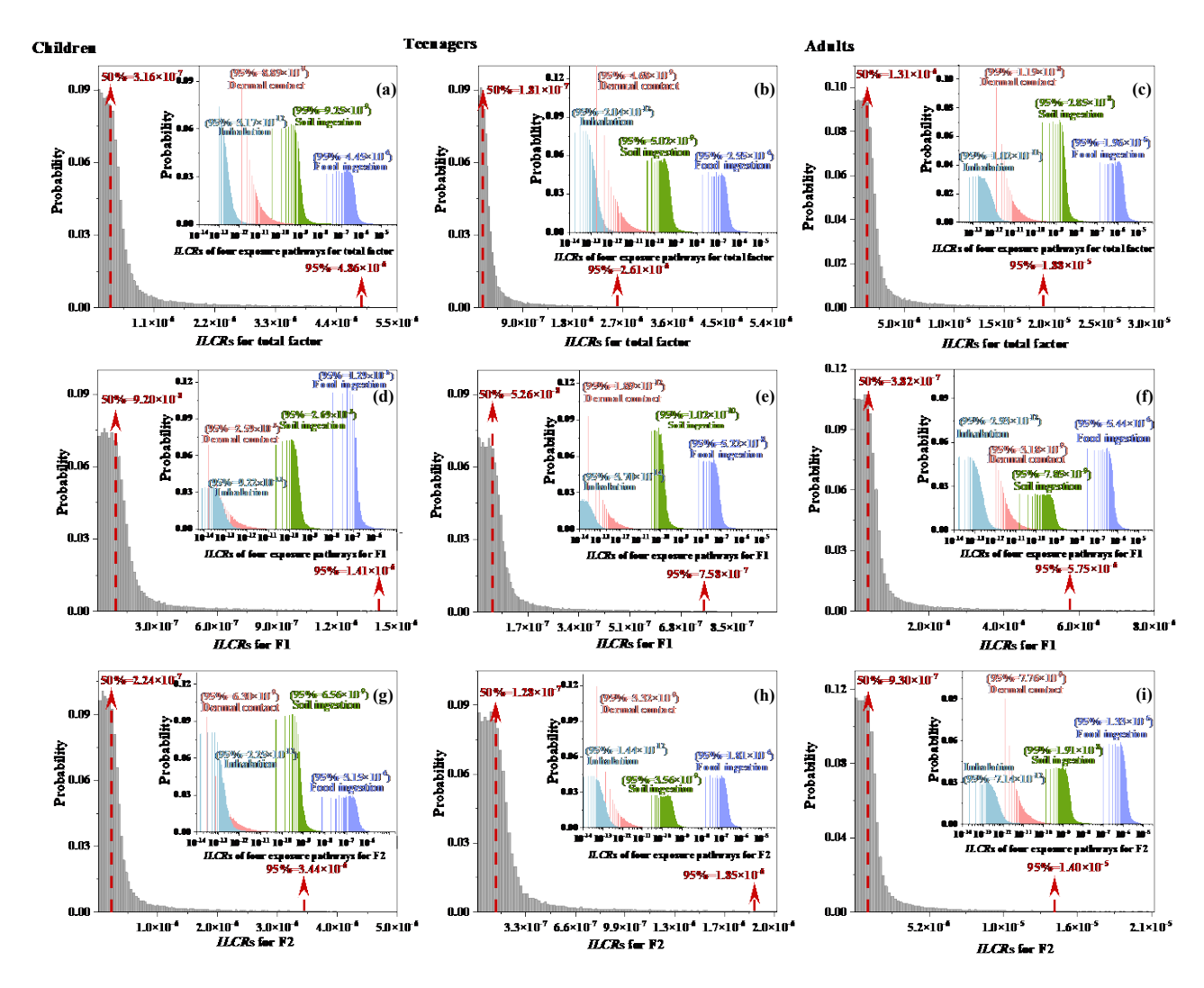


**Fig. 6.** Probability density functions for the carcinogenic risk of soil PAHs in children (a-c), teenagers (d-e), and adults (j-i) were estimated based on the total factor and the two identified pollution sources (F1: coal combustion and vehicle emission sources; F2: petrogenic source).

The carcinogenic risk of PAHs from different sources was further quantified based on the contribution of the sources identified by APCS-MLR. The carcinogenic risk from petrogenic sources was higher than that from coal combustion/vehicle emission sources for all age groups (Fig. 6d-i). Although the risk from PAHs released during shale gas exploitation is relatively low, it is essential to continue monitoring and assessing the associated risks, particularly for adult populations, since the intensity of shale gas development is expected to increase due to advancements in technology

and growing market demands.

Key parameters contributing to *ILCR* were further identified through sensitivity analyses. Exposure time (*ED*) was the most influential variable, with correlation coefficients of 0.704, 0.715, and 0.712 for children, teenagers, and adults, respectively (**Fig. S7**). Additionally, the concentrations of 7 carcinogenic PAHs and the carcinogenic slope factor for ingestion (*CSF*<sub>ingestion</sub>) were found to considerably impact the risk. Consistent with previous studies, *ED*, *C*<sub>soil</sub>, and *CSF*<sub>ingestion</sub> were identified as the three most sensitive indicators influencing the risk of PAH carcinogenesis in soil<sup>37</sup>. Given the long-term nature of shale gas development and cumulative properties of PAHs in soils, relevant authorities should integrate long-term health risk assessments into shale gas development planning to balance energy pursuits with health protection for residents.

#### 4. Conclusions

This study provides novel evidence that shale gas exploitation activities have elevated PAH concentrations in previously uncontaminated background soils, despite overall concentrations remaining at low to moderate levels when compared to global oil and gas exploitation areas. PAH hotspots in the towns and near shale gas fields were accumulated and primarily driven by anthropogenic activities rather than by secondary distribution of soil physic-chemical properties. The predominant sources were coal combustion/vehicle emission and petrogenic sources, the former primarily affected towns and shale gas field soils, and the latter had a broader impact across the study area. Despite the intensive exploitation, the ecological risk was generally acceptable in the study area, except in some shale gas sites due to intensified activities. Carcinogenic risk of PAHs can be negligible to both children and teenagers but be potentially important to adults. Notably,

petrogenic sources contributed more considerably to ecological and health risks. In the broader environmental context, these findings highlight the need for proactive environmental monitoring in emerging shale gas areas globally, as current "acceptable" ecological risk levels may mask underlying contamination trends that could intensify with continued industrial expansion. The source apportionment methodology and risk assessment framework developed here are transferable to other unconventional energy development areas worldwide, contributing to the global understanding of energy-related environmental hazards. Despite limitations such as the use of non-localized parameters for risk assessment in Fuling and potential seasonal variations in PAH distribution, the findings provide a robust scientific foundation for implementing targeted risk mitigation strategies to ensure the sustainable coexistence of shale gas exploitation activities, environmental protection and human health.

# **CRediT** authorship contribution statement

Junwu Xiong: Investigation, Methodology, Data curation, Formal analysis, Visualization, Writing-original draft. Xi Fan: Investigation, Methodology, Data curation, Formal analysis, Writing-review & editing. Xiuwen Yang: Methodology, Validation, Visualization, Writing-review & editing. Huanfang Huang: Methodology, Formal analysis, Validation, Writing-review & editing. Chaojie Qin: Methodology, Data curation, Writing-review & editing. Pu Chang: Formal analysis, Visualization, Writing-review & editing. Yuan Zhang: Resources, Writing-review & editing. Dacong Yin: Resources, Writing-review & editing. Huafeng Liu: Formal analysis, Writing-review & editing. Wei Liu: Conceptualization, Investigation, Resources, Funding acquisition, Writing-review & editing. Shihua Qi: Resources, Supervision, Writing-review & editing. Kevin C. Jones:

- Supervision, Writing-review & editing. Wei Chen: Conceptualization, Investigation, Methodology,
- Data curation, Visualization, Supervision, Resources, Funding acquisition, Writing-review & editing.

# **Declaration of competing interest**

The authors declare no competing financial interest.

# Acknowledgments

564

566

- This study was financially supported by the National Key R&D Program of China
- 568 (2019YFC1805502 and 2018YFC1801701), National Natural Science Foundation of China
- 569 (41907327 and 42007178) and Fundamental Research Funds (G1323523063 and G1323523150) for
- 570 the Central Universities, China University of Geosciences (Wuhan). The authors would like to thank
- Mr. JP Zhou and Ms WQ He for their help during sample collection, and Mr. Z Qian, Ms. ZY Wei,
- Ms. JP Yi and Ms. WX Li for their help in the laboratory analysis.

## 573 References

- 574 (1) Woda, J.; Wen, T.; Oakley, D.; Yoxtheimer, D.; Engelder, T.; Castro, M. C.; Brantley, S. L. Detecting and explaining
- 575 why aquifers occasionally become degraded near hydraulically fractured shale gas wells. Proc. Natl. Acad. Sci. U.S.A.
- **2018**, *115* (49), 12349–12358.
- 577 (2) Qin, Z.; Xu, T. Shale gas geological "sweet spot" parameter prediction method and its application based on
- 578 convolutional neural network. *Sci Rep* **2022**, *12* (1), 15405.
- 579 (3) Wei, J.; Duan, H.; Yan, Q. Shale gas: Will it become a new type of clean energy in China? A perspective of
- 580 development potential. J. Clean Prod. 2021, 294, 126257.
- 581 (4) Wang, S.; Tang, X.; Wang, J.; Zhang, B.; Sun, W.; Höök, M. Environmental impacts from conventional and shale
- gas and oil development in China considering regional differences and well depth. Resour. Conserv. Recycl. 2021, 167,
- 583 105368.
- 584 (5) Xie, W.; Tian, L.; Tang, P.; Cui, J.; Wang, T.; Zhu, Y.; Bai, Y.; Tiraferri, A.; Crittenden, J. C.; Liu, B. Shale gas
- wastewater characterization: Comprehensive detection, evaluation of valuable metals, and environmental risks of heavy
- metals and radionuclides. Water Res. 2022, 220, 118703.
- 587 (6) Ji, X.; Tiraferri, A.; Zhang, X.; Liu, P.; Gan, Z.; Crittenden, J. C.; Ma, J.; Liu, B. Dissolved organic matter in complex
- shale gas wastewater analyzed with ESI FT-ICR MS: Typical characteristics and potential of biological treatment. J.

- 589 Hazard. Mater. 2023, 447, 130823.
- 590 (7) Mayfield, E. N.; Cohon, J. L.; Muller, N. Z.; Azevedo, I. M. L.; Robinson, A. L. Cumulative environmental and
- employment impacts of the shale gas boom. *Nat. Sustain.* **2019**, *2*, 1122–1131.
- 592 (8) Vengosh, A.; Jackson, R. B.; Warner, N.; Darrah, T. H.; Kondash, A. A critical review of the risks to water resources
- from unconventional shale gas development and hydraulic fracturing in the United States. *Environ. Sci. Technol.* **2014**,
- 594 48 (15), 8334–8348.
- 595 (9) Orem, W.; Tatu, C.; Varonka, M.; Lerch, H.; Bates, A.; Engle, M.; Crosby, L.; McIntosh, J. Organic substances in
- produced and formation water from unconventional natural gas extraction in coal and shale. Int. J. Coal Geol. 2014,
- 597 *126*, 20–31.
- 598 (10) Paulik, L. B.; Donald, C. E.; Smith, B. W.; Tidwell, L. G.; Hobbie, K. A.; Kincl, L.; Haynes, E. N.; Anderson, K.
- A. Emissions of polycyclic aromatic hydrocarbons from natural gas extraction into air. Environ. Sci. Technol. 2016, 50
- 600 (14), 7921–7929.
- 601 (11) Wu, F.; Zhou, Z.; Zhang, S.; Cheng, F.; Tong, Y.; Li, L.; Zhang, B.; Zeng, X.; Li, H.; Wang, D.; et al. Toxicity
- identification evaluation for hydraulic fracturing flowback and produced water during shale gas exploitation in China:
- Evidence from tissue residues and gene expression. *Water Res.* **2023**, *241*, 120170.
- 604 (12) Xie, B.; Qin, J.; Sun, H.; Wang, S.; Li, X. Release characteristics of polycyclic aromatic hydrocarbons (PAHs)
- leaching from oil-based drilling cuttings. *Chemosphere* **2022**, *291* (Pt 1), 132711.
- 606 (13) Chao, Z.; Chaojie, Q.; Xi, F.; Junpeng, Z.; Zhe, Q.; Xiuwen, Y.; Jiapei, Y.; Yahui, Z.; Wei, L.; Shihua, Q.; et al.
- Distribution, sources and risk assessment of polycyclic aromatic hydrocarbons (PAHs) in water and sediments from the
- Maxi River Basin in Fuling shale gas field, Chongqing. Acta Scientiae Circumstantiae 2024, 44 (04), 133-144. From
- 609 Cnki.
- 610 (14) Friedman, C. L.; Pierce, J. R.; Selin, N. E. Assessing the influence of secondary organic versus primary
- 611 carbonaceous aerosols on long-range atmospheric polycyclic aromatic hydrocarbon transport. Environ. Sci. Technol.
- **2014**, *48* (6), 3293–3302.
- 613 (15) Chen, K.; Wu, F.; Li, L.; Zhang, K.; Huang, J.; Cheng, F.; Yu, Z.; Hicks, A. L.; You, J. Prioritizing organic pollutants
- for shale gas exploitation: Life cycle environmental risk assessments in China and the US. *Environ. Sci. Technol.* **2024**,
- *58* (19), 8149–8160.
- 616 (16) Sofowote, U. M.; McCarry, B. E.; Marvin, C. H. Source apportionment of PAH in hamilton harbour suspended
- sediments: Comparison of two factor analysis methods. *Environ. Sci. Technol.* **2008**, 42 (16), 6007–6014.
- 618 (17) Jones, K. C. Persistent organic pollutants (POPs) and related chemicals in the global environment: Some personal
- 619 reflections. Environ. Sci. Technol. 2021, 55 (14), 9400–9412.
- 620 (18) Li, Y.; Li, Y.; Huang, Y.; He, T.; Jin, R.; Han, M.; He, Y.; Liu, M. An improved hybrid model on source-risk of
- polycyclic aromatic hydrocarbon in soils of the Yangtze River Delta urban agglomeration. Sci. Total Environ. 2023, 857
- 622 (Pt 1), 159336. From NLM.
- 623 (19) Jia, H.; Zhao, S.; Nulaji, G.; Tao, K.; Wang, F.; Sharma, V. K.; Wang, C. Environmentally persistent free radicals
- 624 in soils of past coking sites: Distribution and stabilization. Environ. Sci. Technol. 2017, 51 (11), 6000–6008.
- 625 (20) Zhang, Y.; Shotyk, W.; Pelletier, R.; Zaccone, C.; Noernberg, T.; Mullan-Boudreau, G.; Martin, J. W. Sources,
- spatial-distributions and fluxes of PAH-contaminated dusts in the Athabasca oil sands region. Environ. Int. 2023, 182,
- 627 108335.
- 628 (21) Shakoor Khan, A.; Akbar Khan, S.; Abbasi, A.; Hajjar, D.; Makki, A. A.; Almahasheer, H.; Moursy, A. R. A.;
- Jimenez-Ballesta, R. Characterization of persistent organic contaminants in the atmosphere of Gadani's ship breaking
- yards and its surrounding: Implications for sustainable ship recycling practices. *Environ. Int.* **2024**, *185*, 108531.

- 631 (22) Lima, A.; De Vivo, B.; Cicchella, D.; Cortini, M.; Albanese, S. Multifractal IDW interpolation and fractal filtering
- method in environmental studies: an application on regional stream sediments of (Italy), Campania region. Appl.
- 633 Geochem. 2003, 18 (12), 1853–1865.
- 634 (23) Dung, T. T. T.; Cappuyns, V.; Swennen, R.; Phung, N. K. From geochemical background determination to pollution
- assessment of heavy metals in sediments and soils. Rev. Environ. Sci. Bio-Technol. 2013, 12 (4), 335–353.
- 636 (24) Aboubakar, A.; Douaik, A.; Mewouo, Y. C. M.; Madong, R. C. B. A.; Dahchour, A.; El Hajjaji, S. Determination of
- background values and assessment of pollution and ecological risk of heavy metals in urban agricultural soils of Yaoundé,
- 638 Cameroon. J. Soils Sediments **2021**, 21 (3), 1437–1454.
- 639 (25) Cheng, Q. Spatial and scaling modelling for geochemical anomaly separation. J. Geochem. Explor. 1999, 65 (3),
- 640 175-194.
- 641 (26) Long, E. R.; Macdonald, D. D.; Smith, S. L.; Calder, F. D. Incidence of adverse biological effects within ranges of
- chemical concentrations in marine and estuarine sediments. *Environ. Manage.* 1995, 19.
- 643 (27) Wang, H.; Huang, X.; Kuang, Z.; Zheng, X.; Zhao, M.; Yang, J.; Huang, H.; Fan, Z. Source apportionment and
- human health risk of PAHs accumulated in edible marine organisms: A perspective of "source-organism-human". J.
- 645 Hazard. Mater. 2023, 453, 131372.
- 646 (28) Dai, C.; Han, Y.; Duan, Y.; Lai, X.; Fu, R.; Liu, S.; Leong, K. H.; Tu, Y.; Zhou, L. Review on the contamination and
- remediation of polycyclic aromatic hydrocarbons (PAHs) in coastal soil and sediments. *Environ. Res.* **2022**, *205*, 112423.
- 648 (29) Li, Y.; Bai, H.; Li, Y.; Zhang, X.; Zhang, L.; Zhang, D.; Xu, M.; Zhang, H.; Lu, P. An integrated approach to identify
- the source apportionment of potentially toxic metals in shale gas exploitation area soil, and the associated ecological
- and human health risks. J. Hazard. Mater. 2023, 458, 132006.
- 651 (30) Guo, X.; Cai, X.; Liu, J.; Liu, C.; Cheng, Z.; Gao, B.; Shi, L. Natural gas exploration progress of sinopec during
- the 13th Five-Year Plan and prospect forecast during the 14th Five-Year Plan. *Nat. Gas Ind. B* **2022**, *9* (2), 107–118.
- 653 (31) Guo, X.; Hu, D.; Shu, Z.; Li, Y.; Zheng, A.; Wei, X.; Ni, K.; Zhao, P.; Cai, J. Exploration, development, and
- 654 construction in the Fuling national shale gas demonstration area in Chongqing: Progress and prospects. Nat. Gas Ind. B
- **2023**, *10* (1), 62–72.
- 656 (32) Pu, C.; Xiong, J.; Zhao, R.; Fang, J.; Liao, Y.; Song, O.; Zhang, J.; Zhang, Y.; Liu, H.; Liu, W.; et al. Levels, sources,
- and risk assessment of polycyclic aromatic hydrocarbons (PAHs) in soils of karst trough zone, Central China. J. Hydrol.
- **2022**, *614*, 128568.
- 659 (33) Chen, W.; Zhang, Z.; Zhu, Y.; Wang, X.; Wang, L.; Xiong, J.; Qian, Z.; Xiong, S.; Zhao, R.; Liu, W.; et al.
- Distribution, sources and transport of polycyclic aromatic hydrocarbons (PAHs) in karst spring systems from Western
- 661 Hubei, Central China. *Chemosphere* **2022**, *300*, 134502.
- 662 (34) Yunker, M. B.; Macdonaldb, R. W.; Vingarzanc, R.; Mitchelld, R.; Goyettee, D.; Sylvestrec, S. PAHs in the Fraser
- River basin: a critical appraisal of PAH ratios as indicators of PAH source and composition. Org. Geochem. 2002, 33
- 664 (4), 489–515.
- 665 (35) Thurston, G. D.; Spengler, J. D. A quantitative assessment of source contributions to inhalable particulate matter
- pollution in metropolitan Boston. Atmos. Environ. 1967, 19 (1), 9–25.
- 667 (36) Wang, H.; Liu, D.; Lv, Y.; Wang, W.; Wu, Q.; Huang, L.; Zhu, L. Ecological and health risk assessments of
- polycyclic aromatic hydrocarbons (PAHs) in soils around a petroleum refining plant in China: A quantitative method
- based on the improved hybrid model. J. Hazard. Mater. 2024, 461, 132476.
- 670 (37) Qi, P.; Qu, C.; Albanese, S.; Lima, A.; Cicchella, D.; Hope, D.; Cerino, P.; Pizzolante, A.; Zheng, H.; Li, J.; et al.
- 671 Investigation of polycyclic aromatic hydrocarbons in soils from Caserta provincial territory, southern Italy: Spatial
- distribution, source apportionment, and risk assessment. J. Hazard. Mater. 2020, 383, 121158.

- 673 (38) Song, Q.; Xiao, S.; Zeng, X.; Zhang, B.; Zhu, Z.; Liang, Y.; Yu, Z. Presence of polycyclic aromatic compounds in
- 674 river sediment and surrounding soil: Possible impact from shale gas wastewater. Sci Total Environ 2024, 953, 176186.
- 675 (39) Liu, Z.; Zheng, T.; Chen, Q.; Chen, X.; Xie, Y.; Wang, Y.; Ren, M.; Gao, Z.-q.; Lin, B.; Feng, X. Identification and
- health risk evaluation of soil contaminated by polycyclic aromatic hydrocarbons at shale gas extraction sites based on
- positive matrix factorization. *Chemosphere* **2024**, *356*, 141962.
- 678 (40) MaliszewskaKordybach, B. Polycyclic aromatic hydrocarbons in agricultural soils in Poland: Preliminary proposals
- 679 for criteria to evaluate the level of soil contamination. Appl. Geochem. 1996, 11 (1-2), 121-127, Article; Proceedings
- 680 Paper.
- (41) The National Standards of the People's Republic of China. Soil environmental quality Risk control standard for soil
- contamination of development land (GB 36600-2018), 2018.
- 683 (42) The National Standards of the People's Republic of China. Soil environmental quality Risk control standard for soil
- contamination of agricultural land (GB 15618-2018), 2018.
- 685 (43) Li, X.; Zheng, R.; Bu, Q.; Cai, Q.; Liu, Y.; Lu, Q.; Cui, J. Comparison of PAH content, potential risk in vegetation,
- and bare soil near Daqing oil well and evaluating the effects of soil properties on PAHs. Environ. Sci. Pollut. Res. 2019,
- 687 *26* (24), 25071–25083.
- 688 (44) Fu, X. W.; Li, T. Y.; Ji, L.; Wang, L. L.; Zheng, L. W.; Wang, J. N.; Zhang, Q. Occurrence, sources and health risk
- of polycyclic aromatic hydrocarbons in soils around oil wells in the border regions between oil fields and suburbs.
- 690 Ecotox. Environ. Safe. 2018, 157, 276–284.
- 691 (45) Wu, B.; Guo, S.; Wang, J. Assessment of the human health risk of polycyclic aromatic hydrocarbons in soils from
- areas of crude oil exploitation. *Environ. Res.* **2021**, *193*, 110617.
- 693 (46) Zhang, D.; Wang, J.; Zeng, H. Soil polycyclic aromatic hydrocarbons across urban density zones in Shenzhen,
- 694 China: Occurrences, source apportionments, and spatial risk assessment. *Pedosphere* **2016**, *26* (5), 676–686.
- 695 (47) Qu, C.; Albanese, S.; Lima, A.; Hope, D.; Pond, P.; Fortelli, A.; Romano, N.; Cerino, P.; Pizzolante, A.; De Vivo,
- B. The occurrence of OCPs, PCBs, and PAHs in the soil, air, and bulk deposition of the Naples metropolitan area,
- 697 southern Italy: Implications for sources and environmental processes. *Environ. Int.* **2019**, *124*, 89–97.
- 698 (48) Zhang, S.; Li, H. L.; He, R. J.; Deng, W. Q.; Ma, S. T.; Zhang, X.; Li, G. Y.; An, T. C. Spatial distribution, source
- identification, and human health risk assessment of PAHs and their derivatives in soils nearby the coke plants. Sci. Total
- 700 Environ. 2023, 861.
- 701 (49) Xu, F.; Jiang, C. M.; Liu, Q.; Yang, R.; Li, W. W.; Wei, Y.; Bao, L. L.; Tong, H. J. Source identification of polycyclic
- aromatic hydrocarbons (PAHs) in river sediments within a hilly agricultural watershed of Southwestern China: an
- 703 integrated study based on Pb isotopes and PMF method. Environ. Geochem. Health 2025, 47 (5).
- 704 (50) Du, J. Q.; Liu, J. X.; Jia, T.; Chai, B. F. The relationships between soil physicochemical properties, bacterial
- communities and polycyclic aromatic hydrocarbon concentrations in soils proximal to coking plants. *Environ. Pollut.*
- 706 **2022**, *298*.
- 707 (51) Tang, L.; Gudda, F. O.; Wu, C. X.; Ling, W. T.; El-Ramady, H.; Mosa, A.; Wang, J. Contributions of partition and
- adsorption to polycyclic aromatic hydrocarbons sorption by fractionated soil at different particle sizes. Chemosphere
- 709 **2022**, *301*.
- 710 (52) Nam, J. J.; Thomas, G. O.; Jaward, F. M.; Steinnes, E.; Gustafsson, O.; Jones, K. C. PAHs in background soils from
- Western Europe: Influence of atmospheric deposition and soil organic matter. *Chemosphere* **2008**, 70 (9), 1596–1602.
- 712 (53) Meijer, S. N.; Steinnes, E.; Ockenden, W. A.; Jones, K. C. Influence of environmental variables on the spatial
- distribution of PCBs in Norwegian and UK soils: Implications for global cycling. Environ. Sci. Technol. 2002, 36 (10),
- 714 2146-2153.

- 715 (54) Meijer, S. N.; Ockenden, W. A.; Sweetman, A.; Breivik, K.; Grimalt, J. O.; Jones, K. C. Global distribution and
- budget of PCBs and HCB in background surface soils: Implications or sources and environmental processes. *Environ*.
- 717 Sci. Technol. **2003**, *37* (4), 667–672.
- 718 (55) Lohmann, R.; Northcott, G. L.; Jones, K. C. Assessing the contribution of diffuse domestic burning as a source of
- 719 PCDD/Fs, PCBs, and PAHs to the UK atmosphere. *Environ. Sci. Technol.* **2000**, *34* (14), 2892–2899.
- 720 (56) Agarwal, T.; Khillare, P. S.; Shridhar, V.; Ray, S. Pattern, sources and toxic potential of PAHs in the agricultural
- 721 soils of Delhi, India. J. Hazard. Mater. 2009, 163 (2-3), 1033–1039.
- 722 (57) Simcik, M. F.; Eisenreich, S. J.; Lioy, P. J. Source apportionment and source/sink relationships of PAHs in the
- 723 coastal atmosphere of Chicago and Lake Michigan. Atmos. Environ. 1999, 33 (30), 5071–5079.
- 724 (58) Jadoon, W. A.; Sakugawa, H. Concentrations of polycyclic aromatic hydrocarbons: Their potential health risks and
- sources at three non-urban sites in Japan. J. Environ. Sci. Health Toxic/Hazard. Subst. Environ. Eng. 2016, 51 (11),
- 726 884–899.
- 727 (59) Ishtiaq, J.; Syed, J. H.; Jadoon, W. A.; Hamid, N.; Chaudhry, M. J. I.; Shahnawaz, M.; Nasir, J.; Rizvi, S. H. H.;
- 728 Chakraborty, P.; Li, J.; et al. Atmospheric polycyclic aromatic hydrocarbons (PAHs) at urban settings in Pakistan: Spatial
- variations, sources and health risks. Chemosphere 2021, 274.
- 730 (60) Wild, S. R.; Jones, K. C. Polynuclear aromatic hydrocarbons in the United Kingdom environment: A preliminary
- 731 source inventory and budget. *Environ. Pollut.* **1995**, *88* (1), 91–108.
- 732 (61) Wilson, S. C.; Jones, K. C. Bioremediation of soil contaminated with polynuclear aromatic hydrocarbons (PAHs):
- 733 A review. *Environ. Pollut.* **1993**, *81* (3), 229–249.
- 734 (62) Mebel, A. M.; Landera, A.; Kaiser, R. I. Formation mechanisms of naphthalene and indene: From the interstellar
- 735 medium to combustion flames. J. Phys. Chem. A 2017, 121 (5), 901–926.
- 736 (63) Gudiyella, S.; Buras, Z. J.; Chu, T.-C.; Lengyel, I.; Pannala, S.; Green, W. H. Modeling study of high temperature
- 737 pyrolysis of natural gas. *Ind. Eng. Chem. Res.* **2018**, *57* (22), 7404–7420.
- 738 (64) Nicolini, J.; Khan, M. Y.; Matsui, M.; Cocco, L. C.; Yamamoto, C. I.; Lopes, W. A.; de Andrade, J. B.; Pillon, C.
- N.; Arizaga, G. G.; Mangrich, A. S. Evaluation of PAH contamination in soil treated with solid by-products from shale
- 740 pyrolysis. *Environ. Monit. Assess.* **2015**, *187* (1), 4123.
- 741 (65) Hao, F.; Zou, H.; Lu, Y. Mechanisms of shale gas storage: Implications for shale gas exploration in China. AAPG
- 742 *Bull.* **2013**, *97* (8), 1325–1346.
- 743 (66) McCallum, L. C.; Souweine, K.; McDaniel, M.; Koppe, B.; McFarland, C.; Butler, K.; Ollson, C. A. Health impact
- assessment of an oil drilling project in California. Int. J. Occup. Med. Environ. Health 2016, 29 (2), 229–253.
- 745 (67) Nizzetto, L.; Jarvis, A.; Brivio, P. A.; Jones, K. C.; Di Guardo, A. Seasonality of the air-forest canopy exchange of
- persistent organic pollutants. Environ. Sci. Technol. 2008, 42 (23), 8778–8783.
- 747 (68) McLachlan, M. S.; Horstmann, M. Forests as filters of airborne organic pollutants: A model. *Environ. Sci. Technol.*
- 748 **1998**, *32* (3), 413–420.
- 749 (69) Liao, C. M.; Chiang, K. C. Probabilistic risk assessment for personal exposure to carcinogenic polycyclic aromatic
- hydrocarbons in Taiwanese temples. *Chemosphere* **2006**, *63* (9), 1610–1619.
- 751 (70) Wu, B.; Zhang, Y.; Zhang, X. X.; Cheng, S. P. Health risk assessment of polycyclic aromatic hydrocarbons in the
- source water and drinking water of China: Quantitative analysis based on published monitoring data. Sci. Total Environ.
- **2011**, *410*–*411*, 112–118.

754